GPS/MEMS IMU/UWB tightly coupled integrated navigation with robust Kalman filter based on bifactor[1]

Jiaxing Zhao[1,2], Jian Wang[(✉)1]

1. School of Geomatics and Urban Spatial Informatics, Beijing University of Civil Engineering and Architecture, Beijing, China

2. School of Architecture and Urban Planning, Beijing University of Civil Engineering and Architecture, Beijing, China

✉**: corresponding author,** wangjian@bucea.edu.cn

Abstract：Robust estimation has been extensively employed and developed in the integrated navigation of Global Positioning System (GPS) receivers and Micro-Electro-Mechanical System (MEMS) Inertial Measurement Unit (IMU). To further reduce or even eliminate the influence of abnormal measurements from GPS receivers/MEMS IMU, the range measurements of Ultra-Wideband (UWB) are introduced. This article proposes a GPS/MEMS IMU/UWB tightly coupled integrated navigation with robust Kalman filter based on bifactor. The proposed model consists of two main components: one is the detection of gross errors, which involves constructing an equivalent weight matrix based on bifactor weight elements; and another is estimation, from which the optimal estimation results are obtained. Finally, the simulated test and field test are carried out to verify the proposed model, and the effectively results of the new robust Kalman filter are drawn.

Keywords: Tightly coupled integrated navigation system; Bifactor weight model; Abnormal measurements; Robust estimation

1 Introduction

Global Navigation Satellite System (GNSS) receivers and Micro-Electro-Mechanical System (MEMS IMU) are commonly employed for providing position, velocity and attitude information for moving platform (Han and Wang 2017). Meanwhile, GNSS receivers have been widely used for vehicles navigating with the help of MEMS IMUs or other sensors, which can generally obtain sub-meter-level positioning accuracy in open-sky environments, it faces challenges in urban canyons, tunnels, bridges, and indoor areas where the GNSS signals will be interfered, cut off, or even unavailable (An et. al 2019; Luo and Wang 2017). High-accuracy positioning results will be obtained from GNSS can reduce or eliminate the accumulated systematic errors over time associated with MEMS IMUs (Chen et. al 2021). Ultra-Wideband (UWB) technology has been shown effective in compensating measurement errors and improving positioning performance of GNSS/MEMS IMU integrated systems (Zhang et. al 2020a, 2020b; Wang et. al 2022; Zhong et. al 2020).

Compared with the integration of GNSS and MEMS IMU, an integrated GNSS/MEMS IMU/UWB system (Chen et. al 2021; Zhang et. al 2020a; Sun et. al 2022; Li et. al 2016; Jiang et. al 2021) offers better control the influence of gross errors, and achieves a higher positioning accuracy (Li

et. al 2018). The Kalman filter is commonly used for integrated navigation to obtain optimal estimation, under the assumption of normal distributions for measurement and state vectors. Researchers have developed various models and systems to control the divergence of positioning errors and improve the reliability of state estimation, such as fading adaptive Kalman filtering model, factor graph, adaptive filtering model and robust estimation model (Luo et. al 2017; Yang et. al 2010). Sun et al. (2022) proposed a motion model-assisted GNSS/MEMS IMU integrated navigation system on the basis of a constant yaw rate and velocity (CTRV) model, significantly improving the horizontal accuracy. Zhang et al. (2020a) designed a federal Kalman filtering model for loosely coupled GNSS/IMU/UWB integration system, which can obtain the stable and reliable results, it also can effectively resist the influence of unreliable signals. Navarro et al. (2019) constructed a low-cost GNSS/INS/UWB integration system, it can operate in standalone mode when no additional infrastructure. Jiang et al. (2021) established a tightly coupled GNSS/INS/UWB integrated navigation system, which used the UWB/INS tightly coupled integration to correct the INS accumulation errors with range information from UWB. To eliminate or weaken the influence of gross errors, Li et al. (2016) proposed a tightly coupled GNSS/IMU/UWB integrated navigation system with a robust Kalman filtering model based on Mahalanobis distance, which improved the performance of integrated navigation system. Wang et al. (2016) proposed a tightly coupled GPS/INS/UWB cooperative positioning system, in which the UWB ranging information is used to augment the GPS measurements，which can eliminate the influence of gross errors. Although Yang et al. (2002) constructed a bifactor equivalent weight model based on measurement outliers for GPS survey, its applications in integrated navigation and positioning have been limited (Chen and Shen 2020).

Based on this point, to explore the performance of GPS/MEMS IMU integrated navigation, we designed a GPS/MEMS IMU/UWB tightly coupled integrated navigation system with robust Kalman filter based on bifactor. Accordingly, this article focuses on analyzing the performance and positioning accuracy of GNSS/MEMS IMU/UWB integration system.

2 GPS/MEMS IMU/UWB tightly coupled navigation system

The dynamic model of GPS/MEMS IMU/UWB tightly coupled navigation system is expressed by the following MEMS IMU error equation

$$
\begin{cases}
\delta\dot{\mathbf{r}} = -\omega_{en} \times \delta\mathbf{r} + \delta\mathbf{v} \\
\delta\dot{v} = -\left(2\omega_{ie} + \omega_{en}\right) \times \delta\mathbf{v} - \delta\psi \times f + \eta \\
\delta\dot{\psi} = -\left(\omega_{ie} + \omega_{en}\right) \times \delta\psi + \varepsilon \\
\dot{\eta} = u_\eta \\
\dot{\varepsilon} = u_\varepsilon
\end{cases}
\tag{1}
$$

wherein $\delta\mathbf{r}$、$\delta\mathbf{v}$、$\delta\psi$ stand for the error vectors of position, velocity and orientation, respectively. ω_{en} is the earth rotation angular velocity vector of the geographic coordinate system relative to the coordinate system, ω_{ie} is the rotating angular velocity vector of the earth coordinate system relative to the inertial coordinate system, f is the acceleration force vector and η is the acceleration error vector, and ε is gyroscope drift error vector during the random walk process. u_η and u_ε are Gaussian white noise vectors. The generalized system model can be expressed as follows

$$
\mathbf{X}_k = \mathbf{F}\mathbf{X}_{k-1} + \mathbf{u}_k
\tag{2}
$$

wherein $\mathbf{X}_k$ is an m×1 unknown state vector at time instant t_k, $\mathbf{F}$ is an n×m system transition matrix, $\mathbf{u}_k$ is an n×1 zero-mean Gaussian white noise vector, and the corresponding covariance matrix is Q. The predicted state vector is

$$
\bar{\mathbf{X}}_k = \mathbf{F}\hat{\mathbf{X}}_k
\tag{3}
$$

The measurement model of GPS/MEMS IMU/UWB integrated navigation is defined as follows

$$\mathbf{Z}_k = \mathbf{H}\mathbf{X}_k + \mathbf{\tau}_k \qquad (4)$$

with

$$\mathbf{Z} = \begin{bmatrix} P_j^{\mathrm{GPS}} - P_j^{\mathrm{INS}} \\ D_j^{\mathrm{GPS}} - D_j^{\mathrm{INS}} \\ r_i^{\mathrm{UWB}} - r_i^{\mathrm{INS}} \\ \vdots \end{bmatrix} \qquad (5)$$

wherein P_j^{GPS} and D_j^{GPS} represent the pseudorange and Doppler measurements of the j_{th} GPS satellite. P_j^{INS} and D_j^{INS} stand for the predicted pseudorange and Doppler measurements of the j_{th} GPS satellite by MEMS IMU, r_i^{UWB} is the UWB range measurement by two UWB units. r_i^{INS} is the derivation calculation range by MEMS IMU. $\mathbf{H}$ is an n×m measurement matrix, $\mathbf{\tau}_k$ is the measurement noise vector, which conforms to zero-mean Gaussian white noise with the covariance matrix $\mathbf{R}$. The residual equations of the measurement vector and the predicted state vector are

$$\mathbf{V}_k = \mathbf{H}\hat{\mathbf{X}}_k - \mathbf{Z}_k \qquad (6)$$

$$\mathbf{V}_{\overline{\mathbf{X}}_k} = \hat{\mathbf{X}}_k - \overline{\mathbf{X}}_k \qquad (7)$$

wherein the dimensions of $\mathbf{V}_{\overline{\mathbf{X}}_k}$ and $\mathbf{V}_k$ are m and n, respectively. $\overline{\mathbf{X}}_k$ is the predicted state vector with its covariance matrix $\mathbf{\Sigma}_{k/k-1}$, $\hat{\mathbf{X}}_k$ is the currently estimated state vector, and $\mathbf{Z}_k$ is an n×1 measurement vector with its covariance matrix R_k.

3 Bifactor robust estimation solution

An improved standard Kalman filter, robust Kalman filter based on bifactor, has been developed using the weight matrix of the measured and estimated information. The Least-Squares cost function at the observation epoch *k* is given as follows (Wang et. al 2021)

$$\Omega = \mathbf{V}_k^T \mathbf{R}_k^{-1} \mathbf{V}_k + \mathbf{V}_{\overline{\mathbf{X}}_k}^T \mathbf{\Sigma}_{k/k-1}^{-1} \mathbf{V}_{\overline{\mathbf{X}}_k} = \mathbf{min} \qquad (8)$$

wherein $\overline{\mathbf{P}}$ is called an equivalent weight matrix, $\overline{p}_{ij}$ is an element of the bifactor equivalent weight matrix, γ_{ii} and γ_{jj} are the factors of adaptive equivalent weight elements.

$$\overline{p}_{ij} = p_{ij}\gamma_{ij} \qquad (9)$$

$$\gamma_{ij} = \sqrt{\gamma_{ii}\gamma_{jj}} \qquad (10)$$

The robust Kalman filtering model based on bifactor consists of adaptive factor construction and iteration solutions. The IGG III model is introduced, and the adaptive factors γ_{ii} could be chosen as follows

$$\gamma_{ii} = \begin{cases} 1 & |\tilde{v}_i| \leqslant k_0 \\ \dfrac{k_0}{|\tilde{v}_i|} \dfrac{k_1 - |\tilde{v}_i|}{k_1 - k_0} & k_0 < |\tilde{v}_i| \leqslant k_1 \\ 0 & |\tilde{v}_i| > k_1 \end{cases} \qquad (11)$$

wherein γ_{jj} is the same as γ_{ii}, $\tilde{v}_i$ is a standardized residual vector element for detection the presences of gross errors, when $|\tilde{v}_i| \leqslant k_0$, the gross errors exist. k_1 and k_0 are two constants, usually chosen as $1.0 \sim 1.5$ and $2.5 \sim 8.0$. Then, we obtain the new robust estimation is obtained as follows

$$\hat{\mathbf{X}}_k = (\mathbf{A}^T\mathbf{P}\mathbf{A})^{-1}\mathbf{A}^T\mathbf{P}\mathbf{L}_k \qquad (12)$$

wherein $\mathbf{A} = \begin{bmatrix} \mathbf{H} \\ \mathbf{I}_m \end{bmatrix}$, $\mathbf{L}_k = \begin{bmatrix} \mathbf{Z}_k^T & \overline{\mathbf{X}}_k^T \end{bmatrix}$ and

$\mathbf{P} = \begin{bmatrix} \mathbf{R}_k & \\ & \mathbf{\Sigma}_{k/k-1} \end{bmatrix}$, the matrix $\mathbf{I}_{\mathbf{m}\times\mathbf{m}}$ stands for a m×m unit matrix. The corresponding covariance matrix of the estimated state vector is

$$\mathbf{\Sigma}_{\hat{X}} = \hat{\sigma}_0^2 (\mathbf{A}^T\mathbf{P}\mathbf{A})^{-1} \qquad (13)$$

wherein $\hat{\sigma}_0^2 = \dfrac{\mathbf{V}_k^T \mathbf{R}_k^{-1}\mathbf{V}_k + \mathbf{V}_{\overline{\mathbf{X}}_k}^T \mathbf{\Sigma}_{k/k-1}^{-1}\mathbf{V}_{\overline{\mathbf{X}}_k}}{n}$ is the posteriori variance of unit weight (Wang 2008, 2009).

4 Experiments

To verify the effectiveness of the proposed technique, simulation and field tests were conducted. The field test was carried out on the roof of the Nottingham Geospatial Institute (NGI).

4.1 The simulated test

The simulated test was designed to evaluate the performance of the proposed model. A vehicle is

traveling along a road, and the movement model of the vehicle can be written as

$$x_{k+1} = \begin{bmatrix} 1 & 0 & \mathbf{T} & 0 \\ 0 & 1 & 0 & \mathbf{T} \\ 0 & 0 & 1 & 0 \\ 0 & 0 & 0 & 1 \end{bmatrix} x_k + w_k \qquad (14)$$

$$z_k = \begin{bmatrix} 1 & 0 & 0 & 0 \\ 0 & 1 & 0 & 0 \end{bmatrix} x_k + \tau_k \qquad (15)$$

wherein k represents the epoch time, the 2000 epochs of data were utilized to verify the proposed model, $x_k = [p_N \quad p_E \quad v_N \quad v_E]^T$, p_N and p_E represent the position of the vehicle in the North and East directions, v_N and v_E represent the velocity in the North and East directions, $\mathbf{T}$ represents the sampling step size, w_k represents the process noise, and v_k represents the measurement noise. w_k and v_k obey Gaussian distributions, and y_k represents the measurement position of vehicle. The covariance matrix of the process noise is $Q = diag(4,4,1,1)$, the covariance matrix of the measurement noise is $\mathbf{R} = diag(900,900)$, the initial estimation error covariance matrix is $P_0 = diag(4,4,1,1)$, and the initial state of the vehicle is $x_0 = [1 \quad 1 \quad 0 \quad 0]^T$.

Table 1 RMSE of standard Kalman filter and robust Kalman filter (the simulated test)

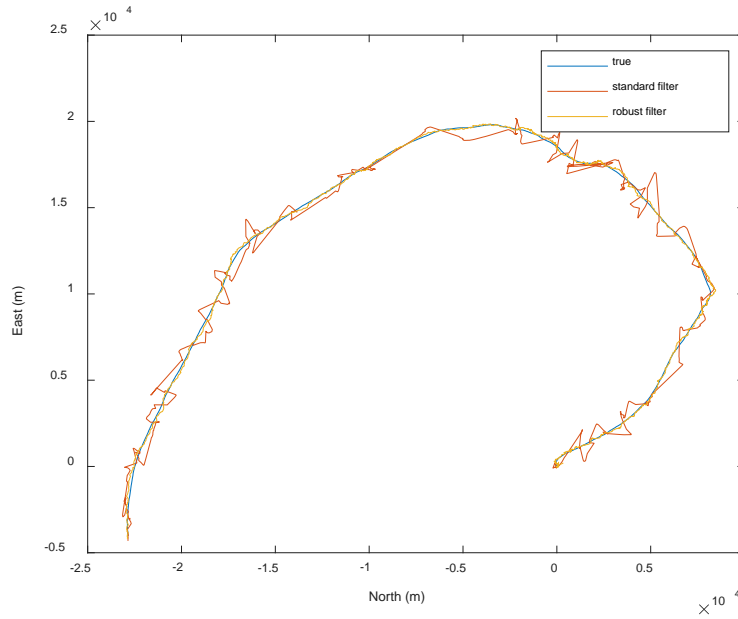|	North (m)	East (m)
Standard Kalman filter	43.86	60.12
Robust Kalman filter (bifactor)	13.11	13.07

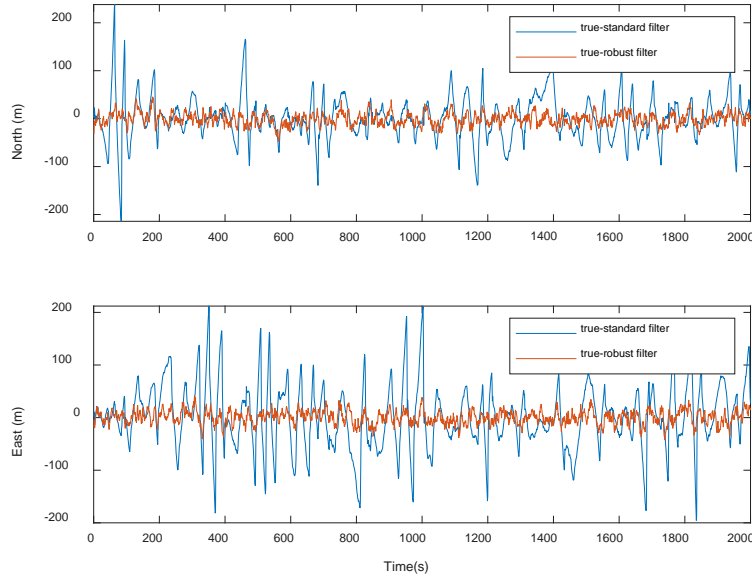Figure 1 Trajectory of vehicle (true, standard and robust filters)

Figure 2 Position error of the vehicle in the North and East directions

Figure 1 shows a simulated test. The position error of a vehicle in the North and East directions are given in Figure 2. In comparison with standard Kalman filter, the robust Kalman filtering model based on bifactor results in a better positioning performance. The Root Mean Squared Error (RMSE) of standard Kalman filter and robust Kalman filter is given in Table 1, which clearly demonstrates that the proposed model significantly improved positioning accuracy in the North and East directions by 70% and 78%.

4.2 Field test

The performance of the proposed model has been evaluated via a field test, and we constructed a GPS/MEMS IMU/UWB tightly coupled integrated navigation with robust Kalman filter based on bifactor. The test consists of one MEMS IMU measurement unit, three UWB measurement units, and two GNSS receivers. One GNSS receiver is mounted on the carrier vehicle, while one UWB unit

was fastened under the antenna with a known lever-arm, another GNSS receiver was set on the roof to act as the reference station, and other two UWB units were mounted on pillars on the roof of NGI, known coordinates, the r_1^{UWB} and r_2^{UWB} ranges were obtained. The duration of the field test is 815 seconds. The number of the tracked satellites was from 6 to 10, with an average is 9 satellites, which meets the basic positioning requirements. Figure 3 illustrates the number of satellites tracked by the GNSS receiver. The detailed description is given in (Wang et.al 2016; Li et.al 2016).

Table 2 RMSE form standard Kalman filter and robust Kalman filter (the field test)

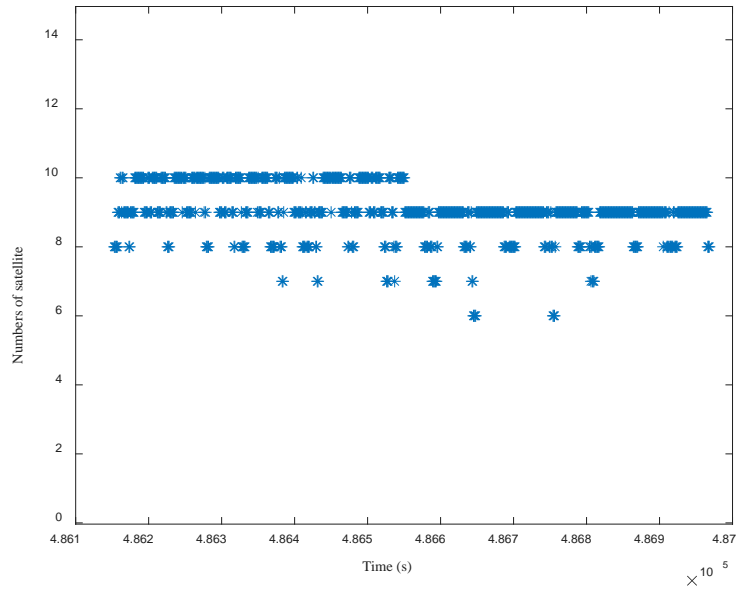|	North (m)	East (m)	Down (m)
Standard Kalman filter	3.29	1.27	1.52
Robust Kalman filter (bifactor)	1.06	0.46	1.29

118

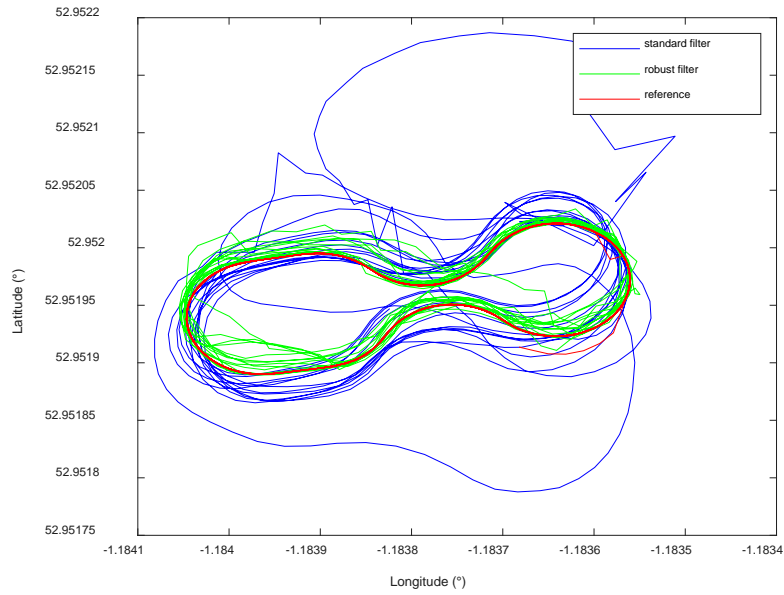Figure 3 Number of satellites tracked by GPS receiver

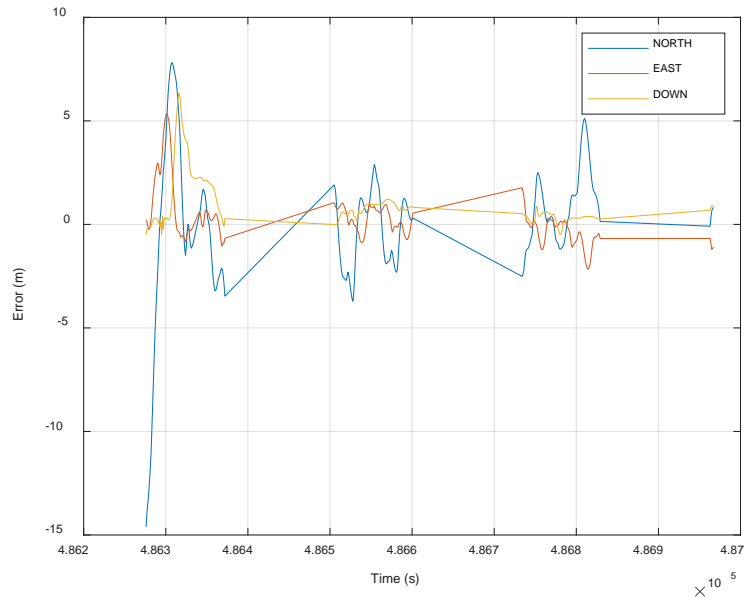Figure 4 Filed trajectory of carrier vehicle

119

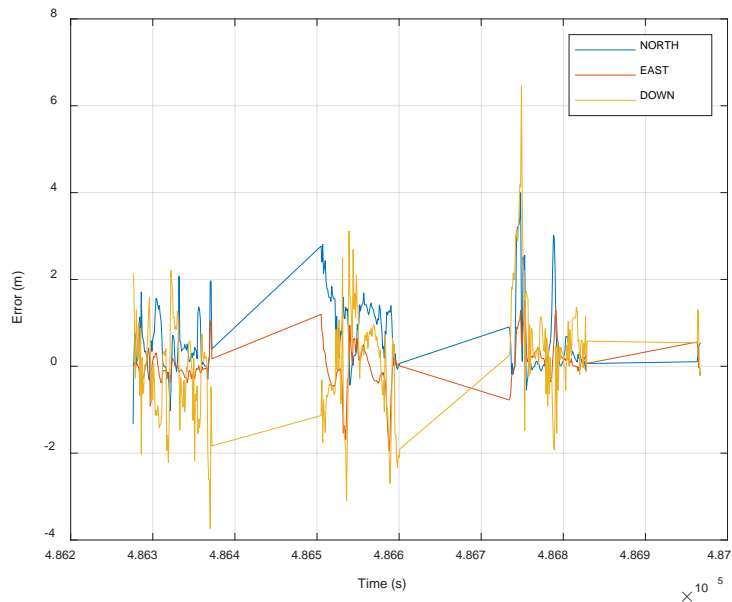Figure 5 Position error of standard Kalman filter

Figure 6 Position error of robust Kalman filter based on bifactor

The simulated test verifies the effectiveness of the robust Kalman filtering model based on bifactor, and the filed test of GPS/MEMS IMU/UWB was conducted to evaluate the performance of proposed model. Figure 4 shows the field test of carrier vehicle in the NGI, with the reference trajectory represented by the red line, the trajectory estimated using the standard Kalman filter represented by the blue line, and the green line trajectory corresponds to the trajectory obtained using the robust Kalman filtering model based on bifactor. Figures 5 and 6 demonstrate the position error of two models in North, East and Down directions. RMSE of different filtering models is shown in Table 2，it clearly presents that the proposed model improved positioning accuracy in the North，East and Down directions by 68%，64%, and 15%，respectively.

5 Conclusion

In this article, we proposed a robust Kalman filtering model based on bifactor for a GPS/MEMS IMU/UWB tightly coupled integrated navigation system. Through the simulated and field tests, the better positioning results were obtained with the proposed model especially in the presence of gross errors in the measurement processing. The proposed model effectively reduced the influence of the outlying measurements. However, it should be noted that this article focused on constructing a tightly coupled integrated navigation system and did not consider various scenarios such as sheltered environments and semi-sheltered environments, which will be addressed in future research endeavors.

Reference

An J, Lee J (2019): Robust positioning and navigation of a mobile robot in an urban environment using a motion estimator, Robotica, 37(8), 1320-1331.

Chen H, Chang L, Xu Z, Ye W, Wu C (2021): UAV collaborative navigation algorithm based on tight combination of GNSS / INS /UWB in complex environment, Chinese Journal of Scientific Instrument, 42(07), 98-107.

Chen J, Shen Y (2020): An Improved Robust Estimation Algorithm for Correlated Observations, Journal of Geodesy and Geodynamics, 40(05): 507-511.

Han H, Wang J (2017): Robust GPS/BDS/INS tightly coupled integration with atmospheric constraints for long-range kinematic positioning, GPS Solutions, 21, 1285-1299.

Jiang W, Cao Z, Cai B, Li B, Wang J (2021): Indoor and outdoor seamless positioning method using UWB enhanced multi-sensor tightly-coupled integration. IEEE Transactions on Vehicular Technology, 70(10), 10633-10645.

Li Z, Chang G, Gao J, Wang J, Hernandez A (2016): GPS/UWB/MEMS-IMU tightly coupled navigation with improved robust Kalman filter, Advances in Space Research, 58(11), 2424-2434.

Navarro M, Arribas J, Vilà-Valls J, Casademont J, Calveras A, Catalán M (2019): Hybrid GNSS/INS/UWB Positioning for Live Demonstration Assisted Driving, 2019 IEEE Intelligent Transportation Systems Conference (ITSC), 3294-3301.

Sun Y, Li Z, Yang Z, Shao K, Chen W (2022): Motion model-assisted GNSS/MEMS IMU integrated navigation system for land vehicle, GPS Solutions, 26(4), 131

Wang C, Xu A, Sui X, Hao Y, Shi Z, Chen Z (2022): A Seamless Navigation System and Applications for Autonomous Vehicles Using a Tightly Coupled GNSS/UWB/INS/Map Integration Scheme, Remote Sens, 14, 27.

Wang J (2008) Test Statistics in Kalman Filtering, Journal of Global Positioning Systems, 7(1):81-90.

Wang J (2009) Reliability Analysis in Kalman Filtering, Journal of Global Positioning Systems, 8(1), 101-111.

Wang J, Boda A, Hu B (2021): Comprehensive error analysis beyond system innovations in Kalman filtering – ScienceDirect, Learning Control, 59-92.

Wang J, Gao Y, Li Z, Meng X, Hancock C (2016): A tightly-coupled GPS/INS/UWB cooperative positioning sensors system supported by V2I communication, Sensors,16(7), 944.

Yang Y, Gao W, Zhang X (2010): Robust Kalman filtering with constraints: a case study for

integrated navigation, Journal of geodesy, 84, 373-381.

Yang Y, Song L, Xu T (2002): Robust estimator for correlated observations based on bifactor equivalent weights, Journal of Geodesy, 76, 353-358.

Zhang R, Shen F, Liang Y, Zhao D (2020a): Using UWB Aided GNSS/INS Integrated Navigation to Bridge GNSS Outages Based on Optimal Anchor Distribution Strategy, 2020 IEEE/ION Position, Location and Navigation Symposium (PLANS), 1405-1411.

Zhang R, Shen F, Li Q (2020b): A Hybrid Indoor/Outdoor Positioning and Orientation Solution Based on INS, UWB and Dual-Antenna RTK-GNSS, 2020 27th Saint Petersburg International Conference on Integrated Navigation Systems (ICINS), 1-5.

Zhong L, Wang R, Wang Y, Ni Y, Liu X, Wang L (2020): Optimizing INS/GNSS/UWB integrated vehicle collaboration navigation based on performance analysis under crowded environments, 2020 3rd International Conference on Unmanned Systems (ICUS), 1042-1046.

Authors

Jiaxing Zhao is currently a Ph.D. candidate at the School of Geomatics and Urban Spatial Informatics, Beijing University of Civil Engineering and Architecture, China. He obtained his M.Sc. degree from Anhui University of Science and Technology in 2021. His current research interests include multi-sensor data fusion for positioning and navigation.

Jian Wang is a professor at Beijing University of Civil Engineering and Architecture, China. He obtained his Ph.D. degree in 2006 from China University of Mining and Technology, China. His current research interests include precise GNSS positioning, GPS/INS and other sensors integrated navigation.